# N-glycosylated molecules act as a co-precipitant in RNA purification

Sungchul Kim[1,§], Yong-geun Choi[1], Kirsten Janssen[2], Christian Büll[3], Bhagyashree S. Joshi[4], Adam Pomorski[4,5] Vered Raz[6], Marvin E. Tanenbaum[4,7], Pascal Miesen[2,§], Zeshi Li[8,§], and Chirlmin Joo[4,9,§]

[1] Center for RNA Research, Institute for Basic Science, Seoul 08826, Republic of Korea
[2] Department of Medical Microbiology, Radboud University Medical Center, 6525 GA Nijmegen, The Netherlands
[3] Department of Biomolecular Chemistry, Institute for Molecules and Materials, Radboud University, 6525 AJ, Nijmegen, The Netherlands
[4] Department of BioNanoScience, Kavli Institute of Nanoscience Delft, Delft University of Technology, 2629 HZ, Delft, The Netherlands
[5] Department of Chemical Biology, Faculty of Biotechnology, University of Wrocław, 50-383, Wrocław, Poland
[6] Human Genetics department, Leiden University Medical Centre, 2333ZC Leiden, The Netherlands
[7] Oncode Institute, Hubrecht Institute–KNAW and University Medical Center Utrecht, 3584 CT Utrecht, The Netherlands
[8] Department of Chemical Biology & Drug Discovery, Utrecht Institute for Pharmaceutical Sciences, Utrecht University, 3584 CG Utrecht, The Netherlands
[9] Department of Physics, Ewha Womans University, Seoul 03760, Republic of Korea
[§] Correspondence: sungchulkim.kr@gmail.com, Pascal.Miesen@radboudumc.nl, z.li@uu.nl, c.joo@tudelft.nl

## Summary

A recent ground-breaking study suggested that small RNA from mammalian cells can undergo N-glycan modifications (termed glycoRNA) [1]. The discovery relied upon a metabolic glycan labeling strategy in combination with commonly used phase-separation-based RNA isolation. Following the reported procedure, we likewise identified an N-glycosylated species in the RNA fraction. However, our results suggest that the reported RNase sensitivity of the glycosylated species depends on the specific RNA purification method. This suggests the possibility of co-purifying unexpected RNase-insensitive N-glycoconjugates during glycoRNA isolation, hinting at the complex biochemical nature of glycoRNA. Our study underscores the need for further research to elucidate the structural and biochemical properties of glycoRNA.

## Introduction

N-linked glycosylation is a major post-translational modification that affects folding, stability, and other cellular functions of secretory and membrane-associated proteins [2]. N-glycosylation starts in endoplasmic reticulum by the assembly of high-mannose glycans and the transfer thereof to nascent peptides. The glycan is then trimmed by ER mannosidases and is further elaborated in the Golgi apparatus, where multi-antennary branching and extension, fucosylation, and sialylation are introduced[3]. Expanding the world of N-glycosylation, a recent study reported that specific small non-coding RNA species in mammalian cells are modified with sialylated and

fucosylated N-glycans [1]. These molecules, referred to as glycoRNA, were reported to localize to the surface of mammalian cells and were shown to interact with either specific Siglec family receptors or P-selectin [1,4,5].

Bioorthogonal labeling of glycans present in RNA isolates was a critical step in the discovery of glycoRNA [1]. Sugar analogs or their precursors modified with bioorthogonal chemistry tags, called metabolic chemical reporters (MCRs), play a crucial role in glycoscience, and enable the delineation of the biogenesis and function of glycosylation. MCR, combined with bioorthogonal labelling, is a popular method due to its simplicity of implementation, the rapidity of the chemical reactions, as well as the bio-compatibility and high specificity in biological environments [6]. MCRs exploit the tolerance of cellular glycan biosynthetic pathways towards unnatural modifications, which are eventually incorporated into glycans [7]. For example, peracetylated N-azidoacetyl-mannosamine ($Ac_4$ManNAz) has been used as MCRs for sialic acid labeling. $Ac_4$ManNAz is converted into azido-sialic acids (SiaNAz) and is normally incorporated at the terminus of glycans [8]. The azide tag in sialoglycans can be conjugated to alkyne-containing molecules, for instance fluorophores or biotin, via copper-catalyzed azide–alkyne cycloaddition (CuAAC) or copper-free strain-promoted alkyne-azide cycloaddition (SPAAC) [9,10]. The latter reaction was used to demonstrate the presence of glycoRNA [1].

SiaNAz-containing glycans in RNA preparations were detected using acidic guanidinium-thiocyanate-phenol-chloroform (AGPC) phase partition [1]. This technique relies on chaotropic agents for cell lysis and protein denaturation, followed by phenol-chloroform-based phase separation for isolation of RNA from cellular components [11,12]. After alcohol precipitation and concentration, RNA is usually further cleaned up using proteases and DNases [12]. To purifiy glycoRNAs, silica-column-based solid-phase extraction for additional purification has employed [1]. This method becomes a common alternative or complementary method to AGPC-based RNA purification as it is believed to yield RNA with higher purity [13]. However, these procedures may introduce artifacts due to incomplete removal of contaminants, such as heparin, during RNA purification [14,15].

Here, we present evidence that may have important implications for the glycoRNA detection. Recapitulating the findings of the previous reports [1,4,5], N-glycosylated molecules were co-purified with RNA during both acidic phenol-chloroform and silica-based column extraction. However, loss of glycoRNA signal in RNA gel electrophoresis upon RNase treatment, which was previously interpreted as the degradation of glycoRNA [1], was apparent only when RNA was isolated using silica columns. Our findings suggest that the RNase sensitivity of glycoRNA observed in the previous reports [1,4,5] is likely a peculiar property introduced during the post-RNase digestion purification steps, only in the use of silica columns. Further strengthening this conclusion, we demonstrate that N-glycosylated molecules may not be covalently linked to RNA but rather co-precipitated with RNA. When RNA molecules were depleted in solution by either RNase treatment or RNA fragmentation, glycoRNA molecules were hardly captured by silica-based columns. However, the addition of RNA or the increase of ethanol percentage in RNA binding buffer recovered the glycoRNA signal. Altogether, our data suggest that RNA isolation methods are susceptible to the presence of specific glycoconjugates. It indicates the potential co-existence of glycoRNAs and unknown N-glycosylated molecules in a complex form, raising intriguing questions about the chemical property of glycoRNA. Our conclusion is based on experiments performed in four laboratories using reagents that were independently purchased.

## Results

### N-glycosylated molecules co-purified with RNA are not RNase-sensitive

To detect glycoRNA, $Ac_4$ManNAz was supplemented in mammalian cell cultures, purified cellular RNA, and conjugated the azide-labeled isolates with dibenzocyclooctyne-biotin (DBCO-biotin) using SPAAC. They visualized SiaNAz-labeled molecules in extracted RNA samples using an RNA (Northern) blotting-like method [1]. This approach can pose several potential complications, such as the use of nitrocellulose membranes for RNA transfer which overall perform less efficiently in RNA detection than positively charged nylon membranes [16,17]. To overcome the limitations of RNA blotting, we developed a simpler approach that eliminated the need for RNA membrane transfer (see methods) and instead relied onlabelling SiaNAz-containing molecules with dibenzocyclooctyne-Cy5 (DBCO-Cy5) for direct fluorescent detection (Fig. 1a). TRIzol reagent was used to remove excess dyes and clean up the RNA sample (Fig. 1a and Extended Data Fig. 1a). This modified method enabled direct in-gel detection of RNA extracted from $Ac_4$ManNAz-treated cells after separation by gel electrophoresis. As expected, no such signal was observed in RNA obtained from DMSO-treated control cells (Fig. 1b). Importantly, the in-gel band pattern was similar to the one observed after transfer to nylon or nitrocellulose membranes, validating that the visualization of N-glycosylated molecules is not affected by the membrane blotting (Extended Data Fig. 1b). We only noted that detection of N-glycosylated molecules was more efficient after transferring to nylon membranes compared to nitrocellulose membranes. Nonetheless, due to its convenience, we used direct in-gel Cy5 detection in further experiments.

To confirm the previous reports of RNase sensitivity and enrichment in small RNA fractions for glycoRNA [1], we included RNA size fractionation using silica columns and enzymatic treatment between dye removal and denaturing agarose gel electrophoresis. In line with the previous findings, the glycan signal was more intense in small RNA than in large RNA fractions, suggesting that the glycosylated moiety mainly co-eluted with small RNA (Fig. 1c). However, surprisingly, we observed that the glycan signal was not affected by either RNase or DNase treatments (Fig. 1c and Extended Data Fig. 1c), raising a question about the biochemical purity of glycoRNA in the conventional extraction methods.

### RNase sensitivity of N-glycosylated molecules is determined by differential purification methods

We sought to find the cause for the observed difference in RNase sensitivity between our findings and those presented in the previous studies [1,5]. In our modified purification method, we minimized the use of silica columns and instead used TRIzol reagent for initial RNA purification, dye removal, and clean-up after enzymatic reactions. Furthermore, we modified the order of experimental steps, performing the click chemistry reaction before enzymatic treatments (“early-click” procedure; Fig. 2a). In comparison, in the procedure of Flynn et al. (2021), all RNA purification steps involved silica columns, and the click chemistry reaction was performed after enzymatic treatments. Finally, the RNA was again column-purified before gel electrophoresis and visualization (“late-click” procedure; Fig. 2a). We speculated that the choice of clean-up strategies could lead to the discrepancy in RNase sensitivity. Therefore, we compared the early-click and late-click procedures side by side. With the early-click approach, we observed strong fluorescent bands of high molecular weight in RNA gel electrophoresis. These bands were insensitive to RNase (Fig. 2b, top left) while the total RNA was efficiently digested by RNase (Fig. 2b,

bottom left). The late-click procedure yielded bands of the same apparent molecular weight but with a much weaker fluorescent signal. Importantly, RNase treatment led to the loss of bands, indicating that RNase sensitivity is affected by the choice of the RNA purification strategy (Fig. 2b, top and bottom right, respectively).

We speculated that the choice of the extraction method at the final purification step was most critical for recovery of glycosylated molecules and the cause for the difference in RNase sensitivity. To test this hypothesis, we kept all protocol steps identical except for the last RNA purification (Fig. 2c). Of note, using our early-click procedure, we found that the recovery of glycoRNA molecules was substantially poorer when silica columns were used to clean up RNA after the enzymatic reaction step. Nonetheless, we observed that RNase treatment led to the loss of glycoRNA signal when RNA was purified with silica columns, but not when TRIzol reagent was used (Fig. 2d and Extended Data Fig. 2a, 2b). Total RNA was efficiently degraded by RNase treatment irrespective of the purification method (Fig. 2d and Extended Data Fig. 2a,b). Taken together, these results indicate that the choice of purification method 'after' the enzymatic reactions results in different recovery of glycan associated molecules.

We note that, regardless of whether RNA was purified with silica columns or TRIzol extraction, the glycan signal was sensitive to the treatment with PNGase F and α2-3,6,8,9 neuraminidase A (Fig. 2d, and Extended Data Fig. 2a,b). PNGase F, is an amidase that cleaves oligomannose-, hybrid-, and complex-type N-glycans from glycoproteins/-peptides [18], and α2-3,6,8,9 Neuraminidase A, which is a sialidase that removes terminal sialic acid residues linked to a penultimate sugar [19]. The glycan signal was also insensitive to proteinase K treatment. Instead, adding proteinase K resulted in the loss of additional bands appearing below the apparant glycoRNA bands (presumably peptide contaminants) in the gel image (Fig. 2e). This suggests that the detected glycosylated molecules in our experiments contain hybrid or complex N-glycans and exhibit the same reactivities towards glycosidases and proteases as reported for glycoRNA [1].

To further scrutinize our interpretation, we applied our approach to various RNases with distinct substrate specificities. While RNase A catalyzes the cleavage of single-stranded RNA (ssRNA) after pyrimidine nucleotides [20], RNase T1 specifically degrades ssRNA at G residues [21]; benzonase can degrade various forms of DNA and RNA [22]; RNase H cleaves RNA in RNA:DNA hybrids [23]; and nuclease P1 hydrolyzes phosphodiester bonds in RNA and ssDNA without base specificity [24]. Our results demonstrated that RNase cocktail, comprising RNase A and T1, and benzonase degraded RNA completely, and RNase T1 and nuclease P1 digested almost all RNA into small pieces, whereas RNase H did not result in RNA degradation (Fig. 2f and Extended Data Fig. 2c). Under all these conditions, labeled molecules remained intact after TRIzol clean-up. However, complete RNA degradation by RNase A, RNase T1, benzonase and nuclease P1 led to the loss of the glycan signal after clean-up using silica columns (Extended Data Fig. 2c). This shows that the presence of RNA is needed for the glycan recovery during late click procedures, irrespective of the choice of nucleases. At this point, to further rule out any potential artifacts arising from the use of the Cy5 dye, we performed the click reaction experiment with DBCO-PEG4-biotin to label metabolically azide-conjugated molecules. Yet, despite following a method similar to the previous studies [1,5], we observed that the enzyme reactivities were fully dependent on RNA isolation strategy [1] (Fig. 2f Extended Data Fig. 2d).

**The efficiency of alcohol precipitation correlates with the recovery of glycoRNA using silica columns**

We set out to understand why glycosylated molecules were poorly recovered when using silica column purification. Our previous observation suggested that linear acrylamide was essential as a co-precipitant in the alcohol precipitation for glycoRNA recovery in the presence of RNase treatment using the early-click protocol (Fig. 2b). This made us speculate that the ethanol percentage and the presence of co-migrating molecules in the binding buffer might be a determinant factor for the efficiency of the glycoRNA capture. Commercially available solid-phase (silica-based) RNA extraction kits use low dielectric constant solvent, like ethanol or isopropanol, for dehydration before silica column binding. This is to reduce the polarity of the aqueous solution [25]. Manufacturers' instructions typically recommend the use of ethanol percentage at around 50% for silica column binding. To investigate if the binding efficiency of glycosylated molecules, including glycoRNAs, to silica columns is enhanced when the ethanol percentage in solutions increases above 50%, we varied the level of ethanol or isopropanol from 20% to 80% and tested the effect of RNase treatment (Fig. 3a). We found that glycosylated molecules were not captured at ethanol concentrations below 40%, regardless of RNase treatment. In line with our previous observations, at 50% ethanol concentration, glycosylated molecules were recovered in untreated conditions but not in the RNase-treated condition (Fig. 3b,c and Extended Data Fig. 3). When the percentage of ethanol and isopropanol increased, glycosylated molecules were recovered more efficiently (Fig. 3b,c and Extended Data Fig. 3). At around 60% ethanol concentrations, the glycosylated signal became visible even in the RNase-treated condition (Fig. 3b, c and Extended Data Fig. 2b and 3). Similar results were obtained when ethanol was replaced with isopropanol (Fig. 3b). The dependency of glycoRNA capture on ethanol or isopropanol percentage has been reported in a recent work [26]. Thus, we concluded that glycoRNA molecules together with unknown glycosylated molecules could be adsorbed into the silica matrix in a dehydration power-dependent manner and speculated that RNA molecules might work as a co-binder to improve the recovery efficiency of glycosylated molecules.

**RNA facilitates the precipitation and adsorption of glycosylated molecules on silica columns**

Our observation indicates that glycosylated molecules in RNA preparations are not digested by RNase but only become less non-specifically adsorbed on silica columns at around 50% ethanol concentration when RNA had been degraded. This led us to the hypothesis that, acting as a co-binder, glycoRNA exists as a complex form with other glycosylated molecules in the purified RNA samples and that the presence of RNA facilitates the adsorption of glycosylated molecules on the silica columns, thereby reducing the contribution from ethanol. In this regard, the recovery of glycosylated molecules, possibly complexed with glycoRNAs, should be restored if exogenous RNA is added to prior RNA-depleted samples. We thus performed a rescue experiment by adding total RNA extracted from unlabeled HeLa cells (i.e., not exposed to $Ac_4$ManNAz) to the RNase treated sample (Fig. 4a). To ensure newly added RNA was not degraded by residual RNase activity, we removed RNase thoroughly by treating samples with proteinase K followed by TRIzol extraction. Strikingly, exogenously added, unlabeled total RNA effectively reduced the required minimum ethanol percentage for binding of of glycosylated molecules to silica columns (Fig. 4b). Adding only one-tenth of the amount of RNA typically present in our RNA preparation was

sufficient to fully restore recovery (Fig. 4b). Similarly, unlabeled RNA from a different cell line (K562) enhanced binding efficiency of glycosylated molecules (Extended Data Fig. 4a,b). Moreover, partially fragmented RNA was sufficient to co-precipitate glycosylated molecules (Extended Data Fig. 4c,d). Only intense RNA fragmentation, which resulted in almost complete RNA degradation, impaired recovery akin to RNase treatment. Notably, adding exogenous total RNA to these fragmented samples rescued the efficient binding of glycosylated molecules to silica matrix (Extended Data Fig. 4e). Interestingly, the addition of plasmid DNA had little effect on the minimum ethanol percentage required for binding of glycosylated molecules to silica (Fig. 4c). These results suggest RNA, but not double-stranded DNA, may specifically interact with glycosylated molecules, leading to their co-isolation in silica-column based extraction methods.

## Discussion

The recent description of N-glycosylated small RNA molecules has shaken our view on the principles of glycosylation and expanded the repertoire of post-transcriptional RNA modifications [1]. Our findings indicate that N-glycosylated molecules are indeed present in RNA preparations from mammalian cells. However, we demonstrated that these N-glycosylated molecules become depleted only in RNase-treated total RNA eluted from silica columns, making it seem like glycoRNA is digested by RNase. This elusive RNase sensitivity does not appear when phenol-chloroform based extraction methods are used. In addition, these molecules are resistant to DNase and proteinases.

This prompted us to investigate the mechanism of non-specific co-purification of glycosylated molecules during silica-column purification. Such molecules bind to the silica matrix even in the absence of RNA when the binding buffer contains ethanol concentrations of 60% or higher or isopropanol. The addition of exogenous RNA enhanced the binding capability of glycosylated molecules to silica columns, indicating that RNA acts as a co-precipitant. Our data demonstrate the co-isolation of RNase-resistant N-glycoconjugates with RNA, and its loss upon RNA removal resemble glycoRNA digestion by RNase.

Therefore, we propose a simple checkpoint experiment for the relevant fields, with which one would be able to tell if the desired molecule is being studied. We suggest one treat the purified, glycan-labeled RNA samples with RNases for an extended period, and then directly load the mixture into the gel electrophoresis, without using a column to clean up the sample. With a transfer to membrane or not, the band at large molecular weight should disappear for glycoRNA. If it does not, one should be alerted that this is likely to be the RNase-resistant N-glycoconjugate.

The biochemical and functional nature of glycoRNA remains to be investigated. N-glycans themselves contain negatively charged moieties, such as sialic acid, phosphate, or sulfate groups [29-34], which enables N-glycosylated molecules to run towards the positive electrode during gel electrophoresis and more efficient transfer to a positively charged nylon membrane. Thus, potential candidates of these molecules may be N-glycosylated oligopeptide products degraded from glycoproteins, which cannot be further cleaved by proteinase K or in which N-glycan protects peptides from further digestion by proteinase K. The possible peptidic nature of glycoRNA-associated glycosylated molecules is supported by the cleavage of an N-glycan from asparagine residues by

PNGase F, which requires at least a tripeptide-containing substrate [35]. However, it is unlikely that glycosylated molecules contain long polypeptide since proteinase K treatment did not affect the band position and intensity of glycosylated molecules during gel electrophoresis (Fig. 2e). Interestingly, a highly hydrophilic oligopeptide containing a sialylated complex-type N-glycan linked to a hexapeptide can be isolated from chicken egg yolk in considerable quantity and high homogeneity [36]. It is thus intriguing to ask if similar molecules also exist in mammalian cells.

Of general importance, our findings demonstrate that even the gold standard RNA purification methods are susceptible to seemingly inert molecules such as glycans which are not easily detected by conventional means. It should be brought to the attention that co-isolation of other biomolecules with extracted nucleic acids are not uncommon. For example, anti-coagulant heparin often contaminates purified DNA or RNA samples from blood collection and plasma processing procedures, and such contamination can complicate reverse transcription and PCR analysis [14,15]. It is currently unclear how glycosylated molecules may have affected and will affect studies that have relied on conventional RNA isolation methods. Our work prompts the development of more reliable RNA purification and post-transcriptional modification methods and will serve as a catalyst for further investigation into a potentially novel biomolecule.

## METHODS

### Key resources table

| Reagent or resource | Source | Identifier |
|---|---|---|
| **Chemicals, peptides, and recombinant proteins** | | |
| Dulbecco's Modified Eagle's Medium (DMEM), high glucose with L-glutamine, sodium pyruvate and sodium bicarbonate | Welgene | Cat# LM001-17 |
| Dulbecco's Modified Eagle's Medium (DMEM) | Gibco | Cat# 41965-039 |
| Fetal bovine serum | Welgene | Cat# S001-01 |
| Fetal bovine serum | Sigma-Aldrich | Cat# F7524 |
| HyClone Characterized Fetal Bovine Serum | Cytiva | Cat# SH30071.03HI |
| Penicillin/streptomycin | Sigma-Aldrich | Cat# P4458 |
| Dulbecco's modified phosphate buffered saline (D-PBS), without calcium chloride and magnesium chloride | Welgene | Cat# LB001-02 |
| Phosphate buffered saline (PBS) | In-house preparation | |
| Dimethyl sulfoxide (DMSO) | Sigma-Aldrich | Cat# 276855 |
| Dimethyl sulfoxide (DMSO) | Merck | Cat# 1.0295.1000 |
| N-azidoacetylmannosamine-tetraacylated ($Ac_4$ManNAz) | Sigma-Aldrich | Cat# 900917-50MG |

| | | |
|---|---|---|
| N-azidoacetylmannosamine-tetraacylated ($Ac_4$ManNAz) | Custom synthesis by Synvenio | |
| TRIzol™ Reagent | Thermo Fisher Scientific | Cat# 15596018 |
| TRI Reagent™ Solution | Thermo Fisher Scientific | Cat# AM9738 |
| TRIzol™ LS Reagent | Thermo Fisher Scientific | Cat# 10296028 |
| Chloroform | Sigma-Aldrich | Cat# C2432 |
| TURBO™ DNase (2 U/µL) | Thermo Fisher Scientific | Cat# AM2238 |
| DNase I (RNase free; 2U/µl) | Thermo Fisher Scientific | Cat# AM2222 |
| RNase A (DNase and protease-free, 10 mg/mL) | Thermo Fisher Scientific | Cat# EN0531 |
| PureLink™ RNase A (20 mg/mL) | Thermo Fisher Scientific | Cat# 12091021 |
| Rapid PNGase F | New England Biolabs | Cat# P0710S |
| α2-3,6,8,9 Neuraminidase A | New England Biolabs | Cat# P0722S |
| Proteinase K, Recombinant, PCR grade | Roche | Cat# 3115879001 |
| Proteinase K | Thermo Fischer Scientific | Cat# AM2548 |
| RNase T1 | Thermo Fischer Scientific | Cat# AM2283 |
| RNase cocktail | Thermo Fischer Scientific | Cat# AM2286 |
| Benzonase® Nuclease | Merck | Cat# E1014-25KU |
| RNase H | New England Biolabs | Cat# M0297L |
| Nuclease P1 | New England Biolabs | Cat# M0660S |
| UltraPure™ Formamide | Thermo Fisher Scientific | Cat# 15515026 |
| UltraPure™ 0.5M EDTA, pH 8.0 | Thermo Fisher Scientific | Cat# 15575020 |
| DEPC-Treated $H_2O$ | Thermo Fisher Scientific | Cat# AM9920 |
| Isopropanol, Optima LC/MS Grade | Fisher Scientific | Cat# A461-500 |
| Ethyl alcohol, Pure | Sigma-Aldrich | Cat# E7023-1L |
| dibenzocyclooctyne-Cy5 (DBCO-Cy5) | Sigma-Aldrich | Cat# 777374-5MG |
| dibenzocyclooctyne-PEG4-biotin (DBCO-biotin) | Sigma-Aldrich | Cat# 760749-5MG |
| Linear acrylamide | Thermo Fisher Scientific | Cat# AM9520 |
| SeaKem® LE Agarose | Lonza | Cat# 50004 |
| NorthernMax® Denaturing Gel Buffer (10X) | Thermo Fisher Scientific | Cat# AM8676 |
| NorthernMax® 10X Running Buffer | Thermo Fisher Scientific | Cat# AM8671 |
| NorthernMax® Transfer Buffer | Thermo Fisher Scientific | Cat# AM8672 |
| Odyssey Blocking Buffer (PBS) | Li-Cor Biosciences | Cat# 927-40000 |
| IRDye 800CW Streptavidin | Li-Cor Biosciences | Cat# 926-32230 |
| MOPS | Sigma-Aldrich | Cat# M1254 |

| | | |
|---|---|---|
| PBS Tablets | Gibco | Cat# 18912-014 |
| TWEEN® 20 | Sigma-Aldrich | Cat# P7949 |
| Sodium Acetate·3$H_2O$ | Merck | Cat# 1.06265.1000 |
| EDTA | Sigma-Aldrich | Cat# EDS |
| 37% Formaldehyde solution | Merck | Cat#1.04003.1000 |
| UltraPure™ Ethidium Bromide, 10 mg/mL | Thermo Fisher Scientific | Cat# 15585011 |
| Zeta-Probe® GT Membrane | Bio-Rad | Cat# 1620194 |
| BrightStar™-Plus Positively Charged Nylon Membrane | Thermo Fisher Scientific | Cat# AM10102 |
| Hybond-C nitrocellulose membrane | Cytiva | Cat# RPN303C |
| Amersham™ Protran® nitrocellulose membrane | Merck | Cat# GE10600001 |
| Ambion® 10X RNA Fragmentation Reagent | Thermo Fisher Scientific | Cat# AM8740 |
| **Critical commercial assays** | | |
| NorthernMax™ Kit | Thermo Fisher Scientific | Cat# AM1940 |
| RNA Clean and Concentrator 5 | Zymo Research | Cat# R1013 |
| **Experimental models: cell lines** | | |
| HeLa | ATCC | Cat# ATCC-CCL-2 |
| K562 | ATCC | Cat# ATCC-CCL-24 |

**Lead contact**

Further information and requests for resources and reagents should be directed to and will be fulfilled by the Lead Contact, Sungchul Kim (sungchulkim.kr@gmail.com).

**Materials availability**

All unique/stable reagents generated in this study are available from the Lead Contact with a completed Materials Transfer Agreement.

**Experimental Model and Subject Details**

**Mammalian cell culture**

HeLa cells were cultured at 37°C and 5% $CO_2$ in Dulbecco's Modified Eagle's Medium (DMEM, Welgene, Fig. 1b,c, 2b–f, 3b,c and 4b,c and Extended Data Fig. 1b,c, 2a–d, 3a and 4d,e; Gibco, Extended Data Fig. 2b) media supplemented with 10% fetal bovine serum (FBS) (Welgene, Fig. 1b,c, 2b–f 3b,c and 4b,c and Extended Data Fig. 1b,c, 2a,c,d, 3a and 4d,e; Sigma-Aldrich, Extended Data Fig. 2b), and also supplemented with penicillin/streptomycin (P/S) (Sigma-Aldrich, Extended Data Fig. 2b). Cells were maintained in 100-mm cell culture dishes (Fig. 1b,c, 2b–f 3b,c and 4b,c and Extended Data Fig. 1b,c, 2a,c,d, 3a and 4d,e) with 10 mL of culture media or, in T75 flasks (Extended Data Fig. 2b). When reaching confluency, cells were split for sub-

culturing. K562 cells (Extended Data Fig. 4b) were cultured at 37°C and 5% $CO_2$ in RPMI medium 1640 supplemented with 10% FBS (Cytiva) and P/S (Sigma-Aldrich) with shaking at 120 rpm.

## Method details

### Labeling with metabolic chemical reporter

Stocks of 500mM N-azidoacetylmannosamine-tetraacylated ($Ac_4$ManNAz) (Sigma-Aldrich, Fig. 1b,c, 2b–f, 3b,c and 4b,c and Extended Data Fig. 1b,c, 2b–d, 3a and 4b,d,e) were prepared in sterile dimethyl sulfoxide (DMSO) (Sigma-Aldrich). For metabolic labeling, we treated $Ac_4$ManNAz at a final concentration of 100 µM in fresh DMEM supplemented with 10% FBS. After 72 h incubation at 37°C and 5% $CO_2$, cells were washed with Dulbecco's Phosphate-Buffered Saline (D-PBS) (Welgene, Fig. 1b,c, 2b–f, 3b,c and 4b,c and Extended Data Fig. 1b,c, 2b–d, 3a and 4b,d,e) twice and stored in -80°C until total RNA extraction. For experiments shown in Extended Data Fig. 4b, the conditions for metabolic labeling were the same, except for that P/S were added in the media.

For experiments shown in Extended Data Fig. 2b, of 50 mM stocks of $Ac_4$ManNAz (Custom synthesis by Synvenio) were prepared in sterile DMSO (Merck). The metabolic labeling was done with 100 µM $Ac_4$ManNAz. in the DMEM (Gibco) supplemented with 10% FBS (Sigma-Aldrich) and 1% P/S. After 48 h at 37 °C and 5% $CO_2$, cells were washed with PBS (in-house preparation) and then followed by total RNA extraction.

### Total RNA extraction with TRIzol™ Reagent

For experiments shown in Fig. 1b,c, 2b–f, 3b,c and 4b and 4c and Extended Data Fig. 1b,c, 2b–d, 3a and 4b,d,e, 1 mL of TRIzol™ reagent (Thermo Fisher Scientific) was added directly onto a washed cell culture dish. Dishes were rocked thoroughly for 10 min at room temperature to lyse and denature all cells. For extracting total RNA from K562 cells (Extended Data Fig. 4b), the cell pellets washed twice with D-PBS were lysed in TRIzol™ reagent (Thermo Fisher Scientific) with 1 mL for ~$10^7$ cells). Homogenized TRIzol-cell mixtures were scrapped with cell scrapper and then transferred into nuclease-free sterile 1.7 mL microtubes. The tubes were vortexed at least for 5 min until complete homogenization for further denaturation of the intermolecular non-covalent interactions. Phase separation was initiated by adding 200 µL (0.2× volumes) of 100% chloroform (Sigma-Aldrich) into 1-mL TRIzol-dissolved cell mixture, and then vortexed thoroughly for complete homogenization. The homogenates were centrifuged at 16,000×g for 10 min at 4°C. The upper (aqueous) phase was carefully removed, transferred into a nuclease-free sterile 1.7 mL, and then mixed with equal volume of 100% isopropanol (Fisher Scientific) by vortexing. The mixture was centrifuged at 16,000×g for 30 min at 4°C, and the supernatant was carefully discarded. The pellet was washed with 1 mL of ice-cold 75% ethanol (Sigma-Aldrich) twice, and then dried completely. The RNA pellet was dissolved with Milli-Q® (Thermo Fisher Scientific, Fig. 1b,c, 2b–f, 3b,c and 4b,c and Extended Data Fig. 1b,c, 2b–d, 3a and 4b,d,e) $H_2O$ or DEPC-treated $H_2O$ (Thermo Fisher Scientific, Extended Data Fig. 4b), and the concentration was measured using a Nanodrop™ 2000 UV/Vis spectrophotometer (Thermo Fisher Scientific).

For experiments shown in Extended Data Fig. 2b, 6 mL of TRI Reagent Solution (Thermo Fisher

Scientific) was added directly to the washed T75 cell culture flask. Homogenates were vortexed for 1 min at RT followed by incubating the samples 1 min at 37°C. 0.2× volumes of chloroform were added, and phase separation was performed at 16,000×g for 10 min at RT. After adding equal volume of isopropanol, mixtures were incubated for 10 min at 4°C. RNA was precipitated at 16,000×g for 10 min at 4°C, washed twice with 75% ethanol and dissolved in nuclease-free $H_2O$. To obtain highly pure RNA preparations, The isolated RNA was re-purified by adding 1 ml of TRI Reagent Solution (Thermo Fisher Scientific) and repeating the isolation procedure described above.

**Copper-free click chemistry and removal of free ligands**

Strain-promoted alkyne-azide cycloadditions (SPAAC) was performed to probe for azide-containing sialo-conjugates in RNA samples using dibenzocyclooctyne-conjugated cyanine 5 (DBCO-Cy5) (Sigma-Aldrich) dyes or DBCO-biotin (Sigma-Aldrich) as the alkyne-azide cycloaddition. Stocks of 10 mM DBCO-Cy5 or DBCO-biotin were made by dissolving 1 mg of lyophilized DBCO-Cy5 in 82.6 µL or 5 mg of DBCO-biotin in 666.7 µL of DMSO, respectively. 9 µL (typically ~50 µg) of RNA dissolved in $H_2O$ were mixed at first with 10 µL of home-made 2× dye-free RNA loading buffer (df-RLB, 95% formamide, 25 mM EDTA, pH8.0) and added with 1 µL of 10 mM (for final 500 µM) DBCO-Cy5 or DBCO-biotin in a microtube. Samples were incubated at 55°C for 10 min. The reaction was stopped by adding 1 mL of TRIzol™ reagent (Thermo Fisher Scientific) and 200 µL of chloroform (Sigma-Aldrich). Alternatively, for experiments performed in Extended Data Fig. 2b, dye removal was achieved by adding 80 µL of DEPC-treated $H_2O$, 300µl of TRIzol LS Reagent (Thermo Fisher Scientific) and 80 µL of Chloroform (Merck). Samples were centrifuged at 16,000×g for 10 min at 4°C or, for experiments shown in Extended Data Fig. 2b, at 16,000×g for 5 min at room temperature. The upper (aqueous) phase was carefully removed, transferred into a nuclease-free sterile tube. For Fig. 1b,c, 2b–f, 3b,c and 4b,c and Extended Data Fig. 1b,c, 2a–d, 3a and 4b,d,e, samples were mixed with equal volume of 100% isopropanol by vortexing, subsequently centrifuged at 16,000×g for 30 min at 4°C, and the supernatant was carefully discarded. The pellet was washed with 1 mL of ice-cold 75% ethanol twice, and then dried completely. The RNA pellet was dissolved with Milli-Q® $H_2O$ (Fig. 1b,c, 2b–f, 3b,c and 4b,c and Extended Data Fig. 1b,c, 2a–d, 3a and 4d,e) or DEPC-treated $H_2O$ (Extended Data Fig. 4b), and the concentration was measured using the UV/Vis spectrophotometer.

**Enzymatic reactions**

Typically, enzymatic reactions were performed with 10 µg (Fig. 2b–f, 3b,c and 4b,c and Extended Data Fig. 1c, 2a–d, 3a and 4b) or 12 µg (Extended Data Fig. 2b) of labeled RNA at 37°C. To digest RNA, 0.5 µL of RNase A (DNase and protease-free, 10 mg/mL) (Thermo Fisher Scientific, Fig. 2b–f, 3b,c and 4b,c Extended Data Fig. 1c, 2a–d, 3a and 4b; PureLink™ RNase A (20 mg/mL) (Thermo Fisher Scientific, Extended Data Fig. 4b), or 1 µL of RNase T1 (Thermo Fisher Scientific, Fig. 2f and Extended Data Fig. 2c,d), or 1 µL of RNase cocktail (500 U of RNase A and 20,000 U of RNase T1 per mL) (Thermo Fisher Scientific, Fig. 2f and Extended Data Fig. 2c,d) were treated with 1.5 µL of 10× TURBO DNase buffer (Thermo Fisher Scientific) in the sample by adjusting with Milli-Q $H_2O$ to total 15 µL. To degrade DNA, 0.5 µL of TURBO DNase (2,000 U/mL) (Thermo Fisher Scientific, Fig. 2b–f

and Extended Data Fig. 1c and 2a,c,d) or DNase I (2,000 U/mL) (Thermo Fisher Scientific, Extended Data Fig. 2b) were treated with 1.5 µL of 10× DNase buffer in the sample by adjusting with Milli-Q $H_2O$ to total 15 µL. To digest both RNA and DNA, 1 µL of benzonase (250,000 U/mL) (Merck, Fig. 2f and Extended Data Fig. 2c,d) or 1 µL of nuclease P1 (100,000 U/mL) (New England Biolabs, Fig. 2f and Extended Data Fig. 2c,d) were treated with 1.5 of 10× TURBO DNase buffer or nuclease P1 buffer in the sample by adjusting with Milli-Q $H_2O$ to total 15 µL. To digest RNA in DNA/RNA hybrids, 1 µL of RNase H (5,000 U/mL) (New England Biolabs, Fig. 2f and Extended Data Fig. 2c,d) were treated with 1.5 of 10× RNase H buffer in the sample by adjusting with Milli-Q $H_2O$ to total 15 µL. To digest N-glycans, 0.5 µL of Rapid PNGase F (New England Biolabs, Fig. 2d and Extended Data Fig. 2a) were added with 1.5 µL of 10× PNGase F buffer (New England Biolabs) in the sample by adjusting with Milli-Q $H_2O$ to total 15 µL. To cut sialic acid moieties, 0.5 of α2-3,6,8,9 Neuraminidase A (New England Biolabs, Fig. 2d and Extended Data Fig. 2a,b) were added with 1.5 µL of 10× GlycoBuffer 1 (New England Biolabs) in the sample by adjusting with Milli-Q $H_2O$ to total 15 µL. To digest proteins, 1 µL of proteinase K (PK, Roche, 20 mg/mL dissolved in Milli-Q $H_2O$, Fig. 1b,c, 2d–f, 3b,c and 4b,c and Extended Data Fig. 1b,c, 2a–d, 3a and 4b; Thermo Fischer Scientific, 20 mg/mL, Extended Data Fig. 2b) was added either with 1.5 µL of 10× TURBO DNase buffer in the RNA sample by adjusting with Milli-Q $H_2O$ to total 15 µL or directly in the precedent enzymatic reactant. The incubation was done for 30 min or 60 min in cases, but all the results always exhibited complete protein digestion.

**RNA fragmentation**

DBCO-Cy5-labeled RNA was fragmented using Ambion® 10X RNA Fragmentation Reagent (Thermo Fisher Scientific). Samples were incubated in 1× RNA Fragmentation Reagent at 75°C for 15 min for mild reaction (Extended Data Fig. 4d) and at 95°C for 2 h for complete fragmentation (Extended Data Fig. 4e). Fragmented RNA samples were immediately mixed with 2× volumes of RBB and various volumes of 100% ethanol for each sample for the final 40%, 50%, 60% and 70% ethanol as indicated in Extended Data Fig. 4d,e.

**RNA clean-up by acidic phenol-chloroform extraction**

For experiments in Fig. 2b,d,f and Extended Data Fig. 2a,c,d, enzymatically digested samples were mixed thoroughly with 1 mL of TRIzol reagent and 200 µL of 100% chloroform (Sigma-Aldrich) for 10 min at room temperature. The homogenates were centrifuged at 16,000×g for 10 min at 4°C. The upper phase was carefully removed, transferred into a nuclease-free sterile 1.7-mL tube, and then mixed with 1 µL of linear acrylamide (Thermo Fisher Scientific) as a co-precipitant and equal volume of 100% isopropanol by vortexing, subsequently centrifuged at 16,000×g for 30 min at 4°C, and the supernatant was carefully discarded. The pellet was washed with 1 mL of ice-cold 75% ethanol twice, and then dried completely. The pellet was dissolved with Milli-Q® $H_2O$. For experiments in Extended Data Fig. 2b, 20 µg linear acrylamide and TRI Reagent Solution (Thermo Fisher Scientific) were used.

**RNA clean-up and size fractionation by silica-based column purification**

16 µL of PK-digested samples were mixed with 34 µL of Milli-Q $H_2O$ to total 50 µL. 100 µL of RBB and 150 µL of

100% ethanol (Final 50% ethanol) were added by reverse pipetting and vortexed thoroughly. For experiments shown in Extended Data Fig. 2b, the final percentage of EtOH was 60%. The mixtures were transferred into the Zymo-SpinTM IC Column in a 2 mL of collection tube. The columns were centrifuged at 16,000×g for 30 sec at room temperature and the flow-through was discarded. 400 µL of RNA Prep Buffer (RPB) (provided by RNA Clean & Concentrator-5, Zymo Research) were added into the column and then centrifuged at 16,000×g for 30 sec at room temperature followed by discarding the flow-through. 700 µL of RNA Wash Buffer (RWB) (provided by RNA Clean & Concentrator-5, Zymo Research) were added into the column and then centrifuged at 16,000×g for 30 sec at room temperature followed by discarding the flow-through. Add 400 µL of RWB were added into the column and then centrifuged at 16,000×g for 30 sec at room temperature followed by discarding the flow-through. Centrifuge at 16,000×g for 1 min at room temperature again to ensure complete removal of the RWB. The columns were carefully transferred into a new nuclease-free sterile 1.7-mL tube, and 15 µL of Milli-Q $H_2O$ or DEPC-treated $H_2O$ directly to the column matrix and incubate for 3 min. The elution was done by centrifuge at 16,000×g for 3 min at room temperature.

For size fractionation of small (smaller than about 200 nucleotides) versus large (larger than about 200 nucleotides) RNAs, samples mixed with equal volume of 50% RBB in 100% ethanol. The mixture was applied onto the Zymo-SpinTM IC Column and centrifuged at 16,000×g for 1 min at room temperature. Large RNAs bound in the column were purified as described above. Small RNAs in the flow-through were mixed with equal volume of 100% ethanol and then purified as described above.

**Denaturing gel electrophoresis, membrane transfer, and blotting**

Typically, formaldehyde-denaturing 1% agarose gel was made by the following. 0.5 g of agarose powder (Lonza) were mixed in 45 mL of Milli-Q $H_2O$ in the flask by swirling but thoroughly. The flask was heated in the microwave oven until complete melting of the agarose. The flask was removed from the oven and then cooled to 55–60°C. 5 mL of 10× NorthernMax™ Denaturing Gel Buffer (Thermo Fisher Scientific) were added and mixed by swirling in the fume hood. The gel mixture was casted following the instruction provided by the casting apparatus. To prepare loading samples, samples were mixed with equal volume of 2× df-RLB, and then incubated at 95°C for 10 min. The gel was resolved in 1× NorthernMax™ Running Buffer (Thermo Fisher Scientific) at 100 V for 40–50 min. For visualization of the Cy5 fluorescence, the gel was rinsed briefly with Milli-Q $H_2O$ and scanned using the gel imaging system (Bio-Rad ChemiDoc XRS+) in the Cy5 filter channel. For ethidium bromide (EtBr) scanning, the Cy5 scanned gel was stained in the water-dissolved UltraPure™ EtBr (Thermo Fisher Scientific) solution for 30 min at room temperature by rocking. The gel was rinsed with Milli-Q $H_2O$ for 30 min at room temperature by rocking and then scanned in the gel imaging system.

For experiments shown in Extended Data Fig. 2b, 1 g of agarose powder (Roche) was dissolved in 72 mL of Milli-Q $H_2O$. 10 mL of 10× MOPS buffer (200 mM MOPS, 50 mM sodium Acetate·$3H_2O$, 10 mM EDTA, pH 7.0) and 18 mL 37% formaldehyde (Merck) were added and mixed. Purified, enzyme treated, RNA samples were incubated at 95 °C for 5 min followed by a quick transfer and 5 min incubation on ice before gel electrophoresis at 90V. Cy5 fluorescence was visualized using the Amersham Typhoon scanner (GE Healthcare).

For membrane transfer, the electrophoresed gel was scanned in the Cy5 channel and then immediately subjected to the transfer instead of EtBr staining, since the EtBr emission was strongly overlapped with Cy5 visualization during the downstream membrane scanning. NorthernMax™ Transfer Buffer (Thermo Fisher Scientific) was used following the manufacturer's instruction for 2 h. For nylon membranes, Zeta-Probe® GT (Bio-Rad) or BrightStar™-Plus (Thermo Fisher Scientific) membranes were used. For nitrocellulose membranes, Hybond-C (Cytiva) or Amersham™ Protran® (Sigma-Aldrich) membranes were used. The transferred membranes were rinsed briefly with Milli-Q $H_2O$ and scanned immediately in the Cy5 channel using Bio-Rad ChemiDoc XRS+.

After transfer of the gel run with biotinylated samples, membranes were subjected to blocked with Odyssey Blocking Buffer, PBS (Li-Cor Biosciences) for 45 min at room temperature, by skipping EtBr staining and fluorescent imaging. After blocking, membranes were stained for 30 min at room temperature with streptavidin-conjugated IR800 (Li-Cor Biosciences), which was diluted to 1:5,000 in Odyssey Blocking Buffer. Excess IR800-streptavidin was washed from the membranes by four times with 0.1% TWEEN-20 (Sigma-Aldrich) in 1× PBS for 10 min/each at room temperature. Membranes were finally washed once with 1× PBS to remove residual TWEEN-20 before scanning. Fluorescent signals from membranes were scanned on Odyssey Li-Cor Sa scanner (Li-Cor Biosciences) with the software set to auto-detect the signal intensity for both 700 and 800 channels. After scanning, images were adjusted to appropriate contrasts with the Li-Cor software (when appropriate) in the 800 channel and exported.

**Acknowledgements**

This work was supported by Young Scientist Fellowship program of the Institute for Basic Science from the Ministry of Science and ICT of Korea (IBS-R008-D1 to S.K.); by TU Delft-Leiden Health Initiative (V.R, C.J.); by a Dutch Research council (NWO) ENW-XS grant (OCENW.XS21.4.046 to P.M.); by ERC Consolidator grant of the European Research Council (819299 to C.J.).

**Authors contributions**

S.K. and Z.L. made the initial discovery. S.K., C.J. and Z.L. designed the study. S.K., Z.L., P.M., and C.J. jointly supervised the work. S.K., Y.C., K.J., A.P, and Z.L. performed the experiments. S.K., K.J., Z.L., P.M., and C.J co-wrote the manuscript with input from all authors.

**Declaration of interests**

The authors declare no competing interests.

**References**

1 Flynn, R. A. *et al.* Small RNAs are modified with N-glycans and displayed on the surface of living cells. *Cell* **184**, 3109-3124 e3122, doi:10.1016/j.cell.2021.04.023 (2021).

2 Esmail, S. & Manolson, M. F. Advances in understanding N-glycosylation structure, function, and regulation in health and disease. *Eur J Cell Biol* **100**, 151186, doi:10.1016/j.ejcb.2021.151186 (2021).

3 Stanley, P., Moremen, K. W., Lewis, N. E., Taniguchi, N. & Aebi, M. in *Essentials of Glycobiology* (eds A. Varki *et al.*) 103-116 (2022).

4 Ma, Y. *et al.* Spatial imaging of glycoRNA in single cells with ARPLA. *Nat Biotechnol*, doi:10.1038/s41587-023-01801-z (2023).

5 Zhang, N. *et al.* Cell surface RNAs control neutrophil recruitment. *Cell*, doi:10.1016/j.cell.2023.12.033 (2024).

6 Zhang, X. & Zhang, Y. Applications of azide-based bioorthogonal click chemistry in glycobiology. *Molecules* **18**, 7145-7159, doi:10.3390/molecules18067145 (2013).

7 Pedowitz, N. J. & Pratt, M. R. Design and Synthesis of Metabolic Chemical Reporters for the Visualization and Identification of Glycoproteins. *RSC Chem Biol* **2**, 306-321, doi:10.1039/d1cb00010a (2021).

8 Moons, S. J., Adema, G. J., Derks, M. T., Boltje, T. J. & Bull, C. Sialic acid glycoengineering using N-acetylmannosamine and sialic acid analogs. *Glycobiology* **29**, 433-445, doi:10.1093/glycob/cwz026 (2019).

9 Saxon, E. & Bertozzi, C. R. Cell surface engineering by a modified Staudinger reaction. *Science* **287**, 2007-2010, doi:10.1126/science.287.5460.2007 (2000).

10 Jacobs, C. L. *et al.* Metabolic labeling of glycoproteins with chemical tags through unnatural sialic acid biosynthesis. *Methods Enzymol* **327**, 260-275, doi:10.1016/s0076-6879(00)27282-0 (2000).

11 Chomczynski, P. & Sacchi, N. Single-step method of RNA isolation by acid guanidinium thiocyanate-phenol-chloroform extraction. *Anal Biochem* **162**, 156-159, doi:10.1006/abio.1987.9999 (1987).

12 Chomczynski, P. & Sacchi, N. The single-step method of RNA isolation by acid guanidinium thiocyanate-phenol-chloroform extraction: twenty-something years on. *Nat Protoc* **1**, 581-585, doi:10.1038/nprot.2006.83 (2006).

13 Boom, R. *et al.* Rapid and simple method for purification of nucleic acids. *J Clin Microbiol* **28**, 495-503, doi:10.1128/jcm.28.3.495-503.1990 (1990).

14 Bai, X., Fischer, S., Keshavjee, S. & Liu, M. Heparin interference with reverse transcriptase polymerase chain reaction of RNA extracted from lungs after ischemia-reperfusion. *Transpl Int* **13**, 146-150, doi:10.1007/s001470050306 (2000).

15 Beutler, E., Gelbart, T. & Kuhl, W. Interference of heparin with the polymerase chain reaction. *Biotechniques* **9**, 166 (1990).

16 Khandjian, E. W. UV crosslinking of RNA to nylon membrane enhances hybridization signals. *Mol Biol Rep* **11**, 107-115, doi:10.1007/BF00364822 (1986).

17 Miribel, L. & Arnaud, P. Electrotransfer of proteins following polyacrylamide gel electrophoresis. Nitrocellulose versus nylon membranes. *J Immunol Methods* **107**, 253-259, doi:10.1016/0022-1759(88)90226-8 (1988).

18 Maley, F., Trimble, R. B., Tarentino, A. L. & Plummer, T. H., Jr. Characterization of glycoproteins and their associated oligosaccharides through the use of endoglycosidases. *Anal Biochem* **180**, 195-204, doi:10.1016/0003-2697(89)90115-2 (1989).

19 Iwamori, M., Ohta, Y., Uchida, Y. & Tsukada, Y. Arthrobacter ureafaciens sialidase isoenzymes, L, M1 and M2, cleave fucosyl GM1. *Glycoconj J* **14**, 67-73, doi:10.1023/a:1018513015459 (1997).

20 Volkin, E. & Cohn, W. E. On the structure of ribonucleic acids. II. The products of ribonuclease action. *J Biol*

*Chem* **205**, 767-782 (1953).

21 Pace, C. N., Heinemann, U., Hahn, U. & Saenger, W. Ribonuclease T1: structure, function, and stability. *Angewandte Chemie International Edition in English* **30**, 343-360 (1991).

22 Miller, M. D., Tanner, J., Alpaugh, M., Benedik, M. J. & Krause, K. L. 2.1 A structure of Serratia endonuclease suggests a mechanism for binding to double-stranded DNA. *Nat Struct Biol* **1**, 461-468, doi:10.1038/nsb0794-461 (1994).

23 Moelling, K., Broecker, F. & Kerrigan, J. E. RNase H: specificity, mechanisms of action, and antiviral target. *Methods Mol Biol* **1087**, 71-84, doi:10.1007/978-1-62703-670-2_7 (2014).

24 Fujimoto, M., Kuninaka, A. & Yoshino, H. Purification of a Nuclease from Penicillium citrinum. *Agricultural and Biological Chemistry* **38**, 777-783, doi:10.1080/00021369.1974.10861230 (1974).

25 Hu, W. P., Chen, Y. C. & Chen, W. Y. Improve sample preparation process for miRNA isolation from the culture cells by using silica fiber membrane. *Sci Rep* **10**, 21132, doi:10.1038/s41598-020-78202-8 (2020).

26 Hemberger, H. *et al.* Rapid and sensitive detection of native glycoRNAs. *bioRxiv*, 2023.2002.2026.530106, doi:10.1101/2023.02.26.530106 (2023).

27 Perr, J. *et al.* RNA binding proteins and glycoRNAs form domains on the cell surface for cell penetrating peptide entry. *bioRxiv*, 2023.2009.2004.556039, doi:10.1101/2023.09.04.556039 (2023).

28 Li, J. *et al.* Novel Approach to Enriching Glycosylated RNAs: Specific Capture of GlycoRNAs via Solid-Phase Chemistry. *Anal Chem* **95**, 11969-11977, doi:10.1021/acs.analchem.3c01630 (2023).

29 Wang, J. R. *et al.* A method to identify trace sulfated IgG N-glycans as biomarkers for rheumatoid arthritis. *Nat Commun* **8**, 631, doi:10.1038/s41467-017-00662-w (2017).

30 Sola, R. J. & Griebenow, K. Effects of glycosylation on the stability of protein pharmaceuticals. *J Pharm Sci* **98**, 1223-1245, doi:10.1002/jps.21504 (2009).

31 Kang, J. Y. *et al.* Lysosomal Targeting Enhancement by Conjugation of Glycopeptides Containing Mannose-6-phosphate Glycans Derived from Glyco-engineered Yeast. *Sci Rep* **8**, 8730, doi:10.1038/s41598-018-26913-4 (2018).

32 Park, H. *et al.* Four unreported types of glycans containing mannose-6-phosphate are heterogeneously attached at three sites (including newly found Asn 233) to recombinant human acid alpha-glucosidase that is the only approved treatment for Pompe disease. *Biochem Biophys Res Commun* **495**, 2418-2424, doi:10.1016/j.bbrc.2017.12.101 (2018).

33 She, Y. M., Li, X. & Cyr, T. D. Remarkable Structural Diversity of N-Glycan Sulfation on Influenza Vaccines. *Anal Chem* **91**, 5083-5090, doi:10.1021/acs.analchem.8b05372 (2019).

34 She, Y. M., Farnsworth, A., Li, X. & Cyr, T. D. Topological N-glycosylation and site-specific N-glycan sulfation of influenza proteins in the highly expressed H1N1 candidate vaccines. *Sci Rep* **7**, 10232, doi:10.1038/s41598-017-10714-2 (2017).

35 Fan, J. Q. & Lee, Y. C. Detailed studies on substrate structure requirements of glycoamidases A and F. *J Biol Chem* **272**, 27058-27064, doi:10.1074/jbc.272.43.27058 (1997).

36 Liu, L., Prudden, A. R., Bosman, G. P. & Boons, G. J. Improved isolation and characterization procedure of

519 sialylglycopeptide from egg yolk powder. *Carbohydr Res* **452**, 122-128, doi:10.1016/j.carres.2017.10.001
520 (2017).

521 **Figure legends**

522 **Figure 1. Glycosylated molecules copurified with glycoRNA are insensitive to RNase treatment**

523 **a.** Schematic of an improved experimental procedure for labeling and visualization. **b.** Glycan detection in Cy5
524 channel from a denaturing agarose gel without any enzymatic treatment condition. Dimethyl sulfoxide (DMSO)
525 was used as an Ac4ManNAz untreated control. Ethidium bromide (EtBr) channel imaged on the gel scanner
526 shows RNAs were intact. **c.** Glycan visualization in total RNA from HeLa cells or size fractionated RNAs.

527

528 **Figure 2. RNase sensitivity of glycosylated molecules depends on the RNA extraction method**

529 **a.** Schematic comparison of early-click and late-click protocols. **b.** Glycan detection by early-click and late-click
530 methods. The asterisk indicates the presence of labeled peptide contaminants (see panel **e**) **c.** Schematic
531 representation of experiments in Fig. 2d and 2e. **d.** Comparison of RNA clean-up steps between silica column
532 and TRIzol protocols for glycan visualization. DBCO-Cy5 labeled RNA samples were reacted with TURBO
533 DNase or RNase A or Rapid PNGase F or $\alpha$2-3,6,8,9 neuraminidase A. Data represent one of three replicates. **e.**
534 Glycan visualization with or without proteinase K treatment. **f.** Blotting of biotinylated glycosylated molecules
535 treated with various nucleases using streptavidin-conjugated IR800 dyes on the nitrocellulose membrane. Right,
536 gel image of EtBr-stained RNA samples. Left, fluorescent image using IR800-streptavidin in 800-nm channel.

537

538 **Figure 3. Ethanol percentage and RNA existence are critical for glycosylated molecule binding onto**
539 **silica column**

540 **a.** Schematic of glycan visualization protocol for various ethanol or isopropanol percentage in silica column
541 binding solutions. **b.** Glycan detection in 20–80% ranges of ethanol or isopropanol by 10% increments. **c.**
542 Glycan detection in 40–70% ranges of ethanol by 3% increments.

543

544 **Figure 4. RNA is the co-binder of glycosylated molecules during silica column purification**

545 **a.** Schematic of glycan visualization protocol for RNA or DNA addition in silica column binding solutions. 5
546 µg of total RNA extracted from $Ac_4$ManNAz-treated HeLa cells were subjected to click chemistry per
547 sample. **b.** Glycan detection without or with total RNA addition in RNA-depleted samples. The amounts of
548 added total RNAs extracted from DMSO-treated HeLa cells are indicated. The range of the ethanol
549 concentrations is 40–70%. **c.** Glycan detection without or with plasmid DNA addition in RNA-depleted
550 samples. The amounts of added plasmid DNA are indicated. The range of the ethanol concentration is 40–
551 70%.

552

553 **Extended Data Figure Legends**

554 **Extended Data Fig. 1. Membrane transfer assay for glycan detection, related to Figure 1**

555 **a.** Schematic of the protocol. **b.** Glycan detection in formaldehyde-denaturing agarose gels and transferred

membranes. For nylon membrane, ZetaProbe GT™ from Bio-Rad™ was used. For nitrocellulose membrane, Hybond C™ from AmershamTM was used. **c.** Glycan detection in gels and transferred membranes with RNase or DNase treatments. For nylon membrane, BrightStar-Plus™ from Invitrogen™ was used. For nitrocellulose membrane, Protran™ from Amersham™ was used.

**Extended Data Fig. 2. Comparison between silica-based column and TRIzol purification for the last clean-up step, related to Figure 2**

**a.** Data represent other two replicates done in Fig. 2d. **b.** Independent comparison from Miesen's experiments for the effect of TRI Reagent and silica column purification on recovery. Final RNA purification in the silica column was performed at 60% EtOH. DNase I was used as an alternative for DNA degradation. **c.** Glycan detection after various nucleases. **d.** Blotting of biotinylated glycans using streptavidin-conjugated IR800 dyes on the nylon membrane. Right, gel image of EtBr-stained RNA samples. Left, fluorescent image using IR800-streptavidin in 800-nm channel.

**Extended Data Fig. 3. Recovery of glycosylated molecules at various ethanol percentages, related to Figure 3**

**a.** Data represent other two replicates done in Fig. 3c. **b.** Relative glycan intensity calculated from the data points in Fig. 3c and Extended Data Fig. 3a. Error bars represent s.d.

**Extended Data Fig. 4. Added RNA but not DNA improves the recovery rate of glycosylated molecules in RNA-depleted conditions, related to Figure 4**

**a.** Schematic for the experiment in Extended Data Fig. 4b. **b.** Data from the Li's experiment. Total RNA extracted from K562 cells was used as an alternative for added HeLa total RNA. **c.** Schematic for experiments in Extended Data Fig. 4d and 4e. **d.** Glycan recovery by the added RNA in the mild RNA fragmentation condition. Partially fragmented RNAs are indicated in EtBr channel. **e**. Glycan recovery by the added RNA in the complete RNA fragmentation condition

# Figure 1

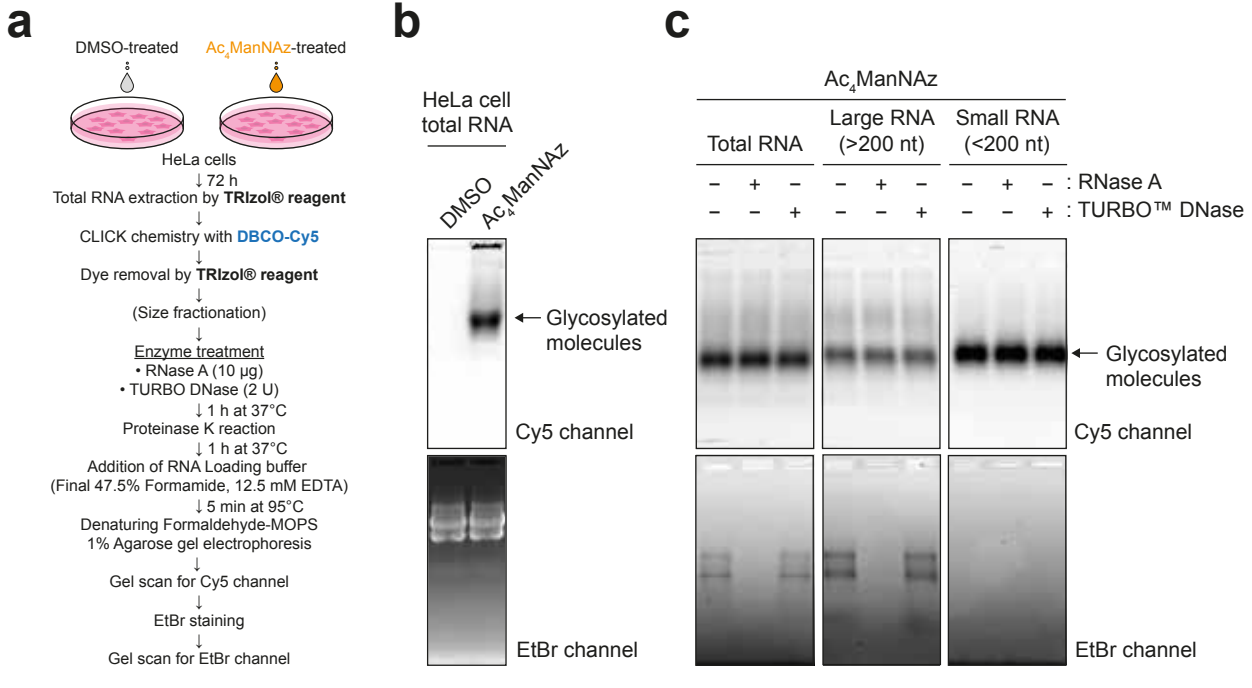
a
DMSO-treated
Ac4ManNAz-treated
HeLa cells
↓ 72 h
Total RNA extraction by TRIzol® reagent
↓
CLICK chemistry with DBCO-Cy5
↓
Dye removal by TRIzol® reagent
↓
(Size fractionation)
↓
Enzyme treatment
• RNase A (10 μg)
• TURBO DNase (2 U)
↓ 1 h at 37°C
Proteinase K reaction
↓ 1 h at 37°C
Addition of RNA Loading buffer
(Final 47.5% Formamide, 12.5 mM EDTA)
↓ 5 min at 95°C
Denaturing Formaldehyde-MOPS
1% Agarose gel electrophoresis
↓
Gel scan for Cy5 channel
↓
EtBr staining
↓
Gel scan for EtBr channel
b
HeLa cell total RNA
DMSO
Ac4ManNAz
← Glycosylated molecules
Cy5 channel
EtBr channel
c
Ac4ManNAz
Total RNA
Large RNA (>200 nt)
Small RNA (<200 nt)
− + − − + − − + − : RNase A
− − + − − + − − + : TURBO™ DNase
← Glycosylated molecules
Cy5 channel
EtBr channel

Figure 2

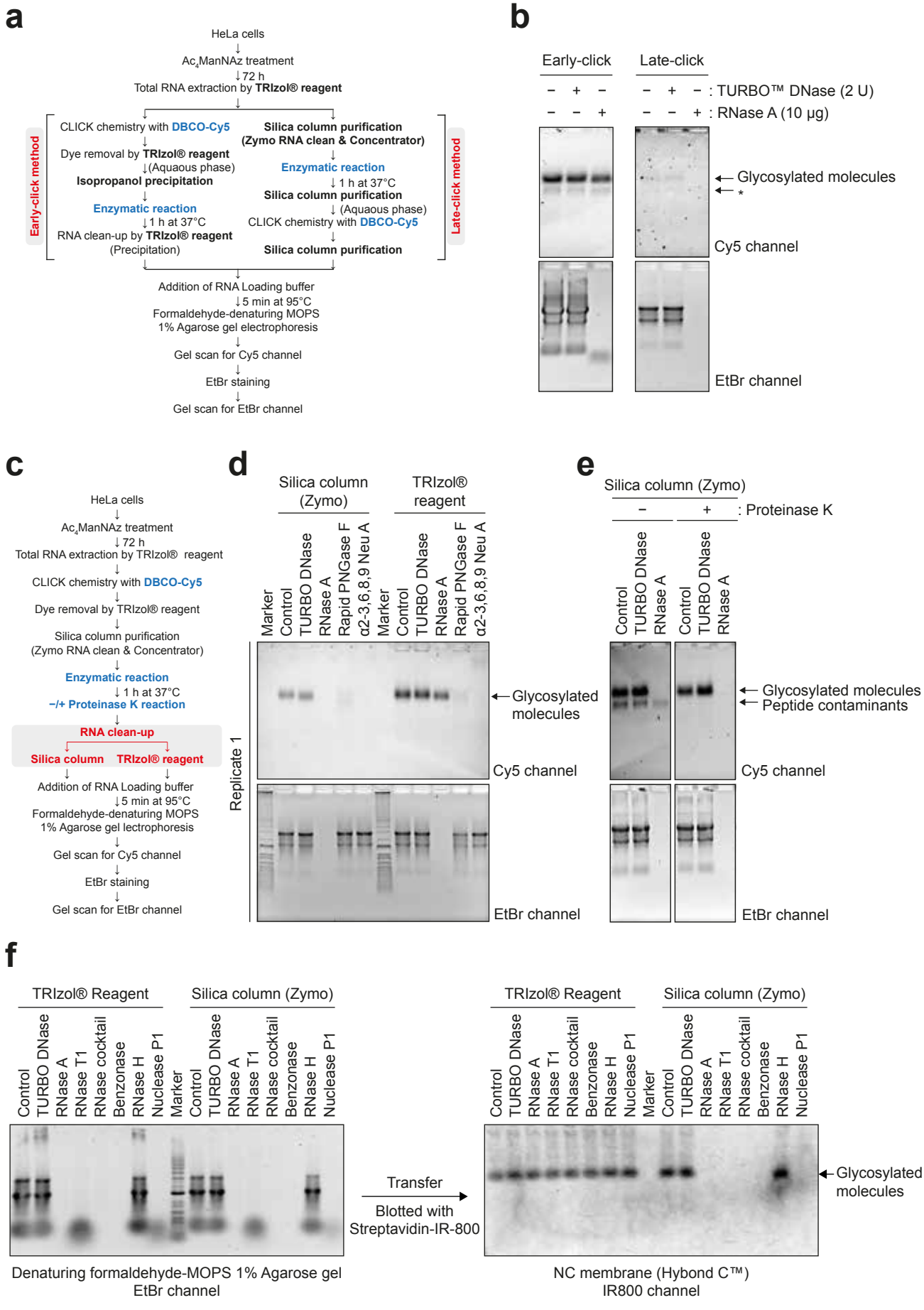
a
HeLa cells
Ac4ManNAz treatment
72 h
Total RNA extraction by TRIzol® reagent
Early-click method
CLICK chemistry with DBCO-Cy5
Dye removal by TRIzol® reagent
(Aquaous phase)
Isopropanol precipitation
Enzymatic reaction
1 h at 37°C
RNA clean-up by TRIzol® reagent
(Precipitation)
Late-click method
Silica column purification
(Zymo RNA clean & Concentrator)
Enzymatic reaction
1 h at 37°C
Silica column purification
(Aquaous phase)
CLICK chemistry with DBCO-Cy5
Silica column purification
Addition of RNA Loading buffer
5 min at 95°C
Formaldehyde-denaturing MOPS
1% Agarose gel electrophoresis
Gel scan for Cy5 channel
EtBr staining
Gel scan for EtBr channel
b
Early-click
Late-click
TURBO™ DNase (2 U)
RNase A (10 µg)
Glycosylated molecules
*
Cy5 channel
EtBr channel
c
HeLa cells
Ac4ManNAz treatment
72 h
Total RNA extraction by TRIzol® reagent
CLICK chemistry with DBCO-Cy5
Dye removal by TRIzol® reagent
Silica column purification
(Zymo RNA clean & Concentrator)
Enzymatic reaction
1 h at 37°C
−/+ Proteinase K reaction
RNA clean-up
Silica column
TRIzol® reagent
Addition of RNA Loading buffer
5 min at 95°C
Formaldehyde-denaturing MOPS
1% Agarose gel lectrophoresis
Gel scan for Cy5 channel
EtBr staining
Gel scan for EtBr channel
d
Silica column (Zymo)
TRIzol® reagent
Marker
Control
TURBO DNase
RNase A
Rapid PNGase F
α2-3,6,8,9 Neu A
Replicate 1
Glycosylated molecules
Cy5 channel
EtBr channel
e
Silica column (Zymo)
Proteinase K
Control
TURBO DNase
RNase A
Glycosylated molecules
Peptide contaminants
Cy5 channel
EtBr channel
f
TRIzol® Reagent
Silica column (Zymo)
Control
TURBO DNase
RNase A
RNase T1
RNase cocktail
Benzonase
RNase H
Nuclease P1
Marker
Transfer
Blotted with Streptavidin-IR-800
Glycosylated molecules
Denaturing formaldehyde-MOPS 1% Agarose gel
EtBr channel
NC membrane (Hybond C™)
IR800 channel

# Figure 3

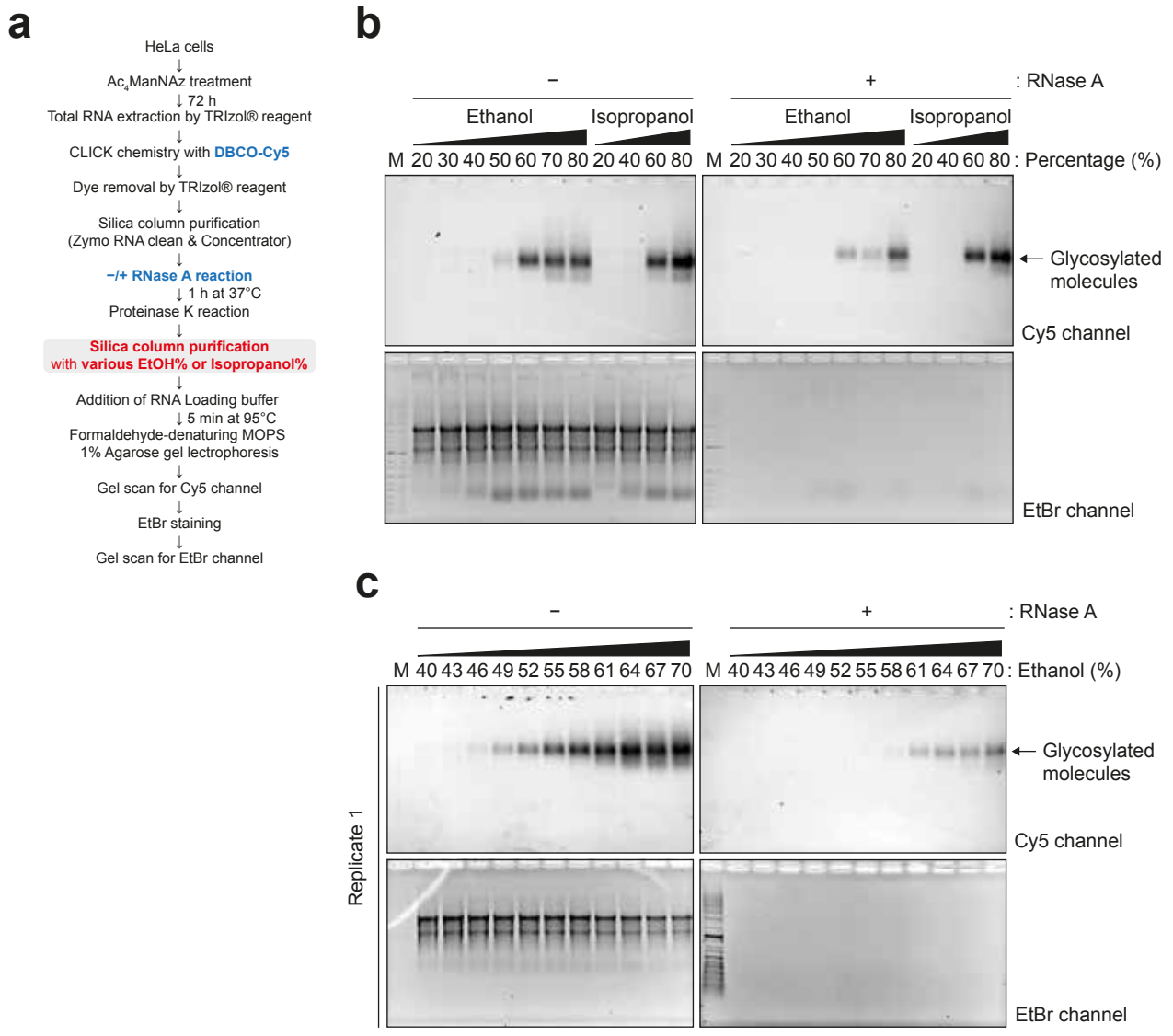
a
HeLa cells
Ac4ManNAz treatment
72 h
Total RNA extraction by TRIzol® reagent
CLICK chemistry with DBCO-Cy5
Dye removal by TRIzol® reagent
Silica column purification
(Zymo RNA clean & Concentrator)
−/+ RNase A reaction
1 h at 37°C
Proteinase K reaction
Silica column purification
with various EtOH% or Isopropanol%
Addition of RNA Loading buffer
5 min at 95°C
Formaldehyde-denaturing MOPS
1% Agarose gel lectrophoresis
Gel scan for Cy5 channel
EtBr staining
Gel scan for EtBr channel
b
−
+
: RNase A
Ethanol
Isopropanol
M 20 30 40 50 60 70 80 20 40 60 80
: Percentage (%)
Glycosylated molecules
Cy5 channel
EtBr channel
c
M 40 43 46 49 52 55 58 61 64 67 70
: Ethanol (%)
Replicate 1

**Figure 4**

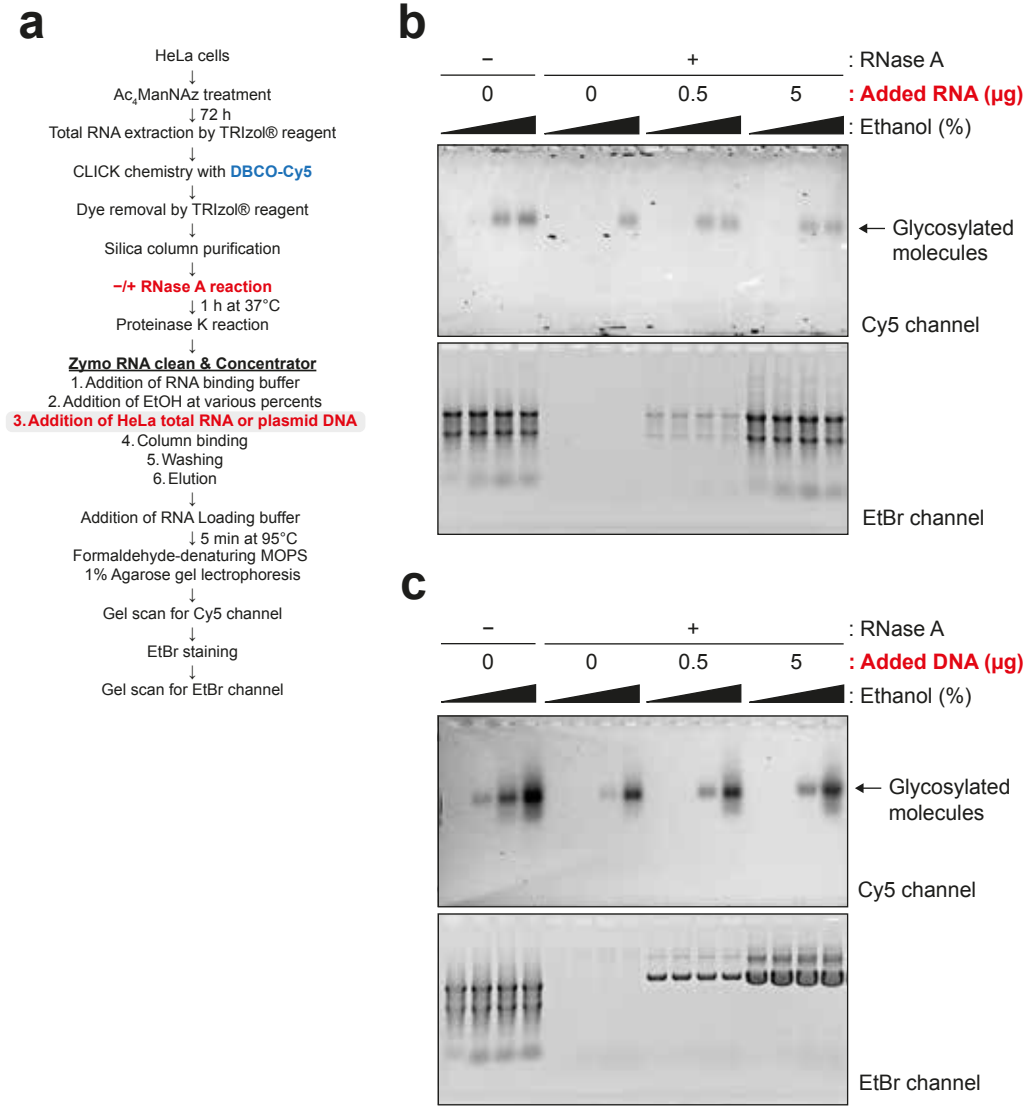
a
HeLa cells
↓
Ac4ManNAz treatment
↓ 72 h
Total RNA extraction by TRIzol® reagent
↓
CLICK chemistry with DBCO-Cy5
↓
Dye removal by TRIzol® reagent
↓
Silica column purification
↓
−/+ RNase A reaction
↓ 1 h at 37°C
Proteinase K reaction
↓
Zymo RNA clean & Concentrator
1. Addition of RNA binding buffer
2. Addition of EtOH at various percents
3. Addition of HeLa total RNA or plasmid DNA
4. Column binding
5. Washing
6. Elution
↓
Addition of RNA Loading buffer
↓ 5 min at 95°C
Formaldehyde-denaturing MOPS
1% Agarose gel lectrophoresis
↓
Gel scan for Cy5 channel
↓
EtBr staining
↓
Gel scan for EtBr channel
b
− + : RNase A
0 0 0.5 5 : Added RNA (μg)
: Ethanol (%)
← Glycosylated molecules
Cy5 channel
EtBr channel
c
− + : RNase A
0 0 0.5 5 : Added DNA (μg)
: Ethanol (%)
← Glycosylated molecules
Cy5 channel
EtBr channel